Fermi National Accelerator Laboratory

FERMILAB-Conf-93/199-E
CDF

The Cross Section for the Production of $b\bar{b}$ Pairs in $p\bar{p}$ Collisions at $\sqrt{s} = 1.8$ TeV

The CDF Collaboration

Fermi National Accelerator Laboratory
P.O. Box 500, Batavia, Illinois 60510

August 1993

Submitted to the *International Symposium on Lepton and Photon Interactions*,
Cornell University, Ithaca, New York, August 10-15, 1993

Operated by Universities Research Association Inc. under Contract No. DE-AC02-76CHO3000 with the United States Department of Energy

Disclaimer

CDF/PUB/BOTTOM/PUBLIC/2166
FERMILAB-CONF-93/199-E

The Cross Section for the Production of $b\bar{b}$ Pairs in $p\bar{p}$ Collisions at $\sqrt{s} = 1.8$ TeV

The CDF Collaboration

Abstract

The cross section for $p\bar{p} \rightarrow b\bar{b}X$ is measured from high mass $e\mu$ events collected with the CDF detector during the 1988-1989 run of the Fermilab Tevatron. Comparisons are made between the data and next-to-leading order (NLO) Quantum Chromodynamics (QCD).

Submitted to International Symposium on Lepton and Photon Interactions,
Cornell University, Ithaca, NY, August 10-15, 1993

Studies of b production in $p\bar{p}$ collisions provide quantitative tests of perturbative QCD. For processes involving squared momentum transfers on the order of m_b^2, the strong coupling constant, α_s, becomes relatively small and perturbative methods are expected to work well. Measurements of the inclusive cross section for $p\bar{p} \rightarrow bX$ have been made at UA1 [1] and at CDF [2]. The NLO QCD prediction [3] is in good agreement with the data at $\sqrt{s} = 630$ GeV but is systematically low when compared to the CDF measurements at $\sqrt{s} = 1.8$ TeV. Consideration of the process $p\bar{p} \rightarrow b\bar{b}X$ provides further opportunities for comparison of experiment and NLO QCD. We examine the P_T correlations between the two quarks by measuring the cross section as a function of the b P_T thresholds. We also investigate spatial correlations by examining the opening angle of the two quarks in the transverse plane.

CDF has been described in detail elsewhere [4]. Here, we mention only those components most relevant to this analysis. The central region[1] ($\mid \eta \mid < 1.1$) is instrumented with a large volume drift chamber surrounded by a 1.4 Tesla superconducting solenoid. The combination provides three dimensional tracking with a momentum resolution of $0.002P_T$, where $P_T = Psin\theta$. The solenoid is followed by the central electromagnetic (CEM) and the central hadronic (CHA) calorimeters. The CEM is a lead-scintillator sandwich with an energy resolution of $13.5\%/\sqrt{E_T}$, where $E_T = Esin\theta$. Imbedded at shower maximum within the CEM are the central electromagnetic strip chambers (CES). The fine segmentation of the CES allows for precise measurements of the

[1] CDF is cylindrically symmetric and is described by a coordinate system in which $+z$ lies along the direction of the proton beam. The azimuthal angle is denoted by ϕ and the polar angle by θ. The pseudorapidity, η, is defined as $-\ln \tan(\theta/2)$.

transverse shower profile in both ϕ and z. The CHA is a steel-scintillator sandwich with $50\%/\sqrt{E_T}$ energy resolution. Muon chambers are located outside the calorimetry, covering the interval $|\eta| < 0.6$.

The data consist of events collected with a dilepton trigger. The trigger requires an electron in the CEM with a minimum E_T of 5 GeV and a muon with a minimum P_T of 3 GeV/c. The data come from $b\bar{b}$ production, $c\bar{c}$ production and 'fakes', where fakes are misidentified or non-prompt particles. To determine the number of $e\mu$ events due to $b\bar{b}$ production, we separate the data into events with leptons of opposite sign (OS) and the same sign (SS). $b\bar{b}$ production produces mostly OS pairs, but also contributes to SS because of $B^0\overline{B^0}$ mixing. $c\bar{c}$ contributes only to OS as there is negligible mixing. Fakes contribute equally to OS and SS. The fake background is removed by subtracting the SS $e\mu$ pairs from the OS. The number of sign subtracted events, $\Delta_{e\mu}$, is equal to the excess OS $b\bar{b}$ events, $\Delta_{b\bar{b}}$, plus the $c\bar{c}$ contribution, $N_{c\bar{c}}$: $\Delta_{e\mu} = \Delta_{b\bar{b}} + N_{c\bar{c}}$. Denoting the fraction of sign-subtracted events due to $b\bar{b}$ as $f_{b\bar{b}}$, $\Delta_{b\bar{b}} = f_{b\bar{b}}\,\Delta_{e\mu}$. The total number of $b\bar{b}$ events, $N_{b\bar{b}}$, is obtained by correcting $\Delta_{b\bar{b}}$ for the number of events lost in the sign subtraction.

$$N_{b\bar{b}} = \frac{f_{b\bar{b}}\Delta_{e\mu}}{(1-2\chi)^2\delta}.$$

The factor, $(1-2\chi)^2$, corrects for the events lost due to mixing. χ is the b mixing

parameter and is defined as:

$$\chi \equiv \frac{Prob(b \rightarrow \overline{B^0} \rightarrow B^0 \rightarrow \ell^+)}{Prob(b \rightarrow \ell^{\pm})}.$$

Here B^0 refers to either B_d^0 or B_s^0. The factor, δ, corrects for a smaller fraction of events lost because of cases in which the leptons are produced in different stages of the B decay chain. Lepton pairs from the decay of a single B are removed from the data by requiring that $M_{e\mu} > 5$ GeV, where $M_{e\mu}$ is the invariant mass of the $e\mu$ pair.

The fraction, $f_{b\bar{b}}$, of the sign subtracted events, $\Delta_{e\mu}$, due to $b\bar{b}$ production is determined by examining the P_T^{rel} distribution. P_T^{rel} is the component of the lepton momentum transverse to the direction of the associated jet. The distribution of P_T^{rel} from b decays is stiffer than the corresponding spectrum from c decays. We obtain the jet axes by clustering tracks with a fixed cone clustering algorithim. The tracks associated with the electron and muon are excluded from the clustering. The shape of the P_T^{rel} distribution for b and c decays is obtained from Monte Carlo. Figure 1 shows the electron P_T^{rel} distributions for OS and SS events. Also shown is the sign-subtracted distribution with a fit to the sum of the normalized b and c distributions; the fit indicates $f_{b\bar{b}} = 1.0^{+0.0}_{-0.1}$.

The cross section for the inclusive production of two b quarks is:

$$\sigma(p\bar{p} \rightarrow b\bar{b}X) = \frac{N_{b\bar{b}}}{\mathcal{L}\varepsilon_{CUTS}\varepsilon_{TRIG}A(e)A(\mu)2Br(b \rightarrow eX)Br(b \rightarrow \mu X)}.$$

$\mathcal{L}$ is the integrated luminosity represented by the data. $A(\ell)$ ($\ell = \mu, e$) is the acceptance for leptons from b decay. ε_{TRIG} is the combined efficiency of the electron and muon trigger requirements. ε_{CUTS} is the combined efficiency of the electron and muon quality cuts.

The efficiencies of the electron cuts are calculated from the data. Since $f_{b\bar{b}}$ is consistent with unity, sign-subtracted distributions of electron related quantities represent electrons from b decay and are used to calculate the efficiencies of the electron quality cuts. The efficiencies of the muon quality cuts are obtained from $J/\psi \rightarrow \mu^+\mu^-$ events.

The electron and muon trigger requirements are uncorrelated and are considered seperately. The efficiency of the muon trigger requirements is obtained from a study of cosmic ray events [5]. The efficiency of the electron requirements is determined from a simulation of the trigger. The simulation is seen to reproduce the efficiency, derived from the data, of a similar electron trigger.

The electron and muon acceptances are calculated using the full NLO calculation of $b\bar{b}$ production by Mangano, Nason, and Ridolfi (MNR) [6]. The acceptances are defined as the fraction of accepted b quarks relative to the number of b quarks with $P_T > P_T^{min}$. P_T^{min} is defined as the P_T such that 90% of the accepted quarks have $P_T > P_T^{min}$. Figure 2 shows the MNR prediction for the P_T^{min} of the second b quark (P_T^{min2}) in an event as a function of the P_T^{min} of the first (P_T^{min1}). The $E_T > 5$ GeV requirement for the electron yields a P_T^{min1} value of 8.75 GeV. Consulting the

$P_T(\mu) >$ (GeV)	3.0	4.0	5.0
P_T^{min} (GeV)	6.5	7.5	8.75
$\Delta_{e\mu}$	248 ± 33	190 ± 25	115 ± 18
ϵ_{TRIG}	0.56 ± 0.08	0.56 ± 0.08	0.60 ± 0.09
ϵ_{CUTS}	0.62 ± 0.21	0.51 ± 0.17	0.40 ± 0.16
$A(\mu)$	0.116 ± 0.021	0.099 ± 0.018	0.092 ± 0.017
δ	0.76 ± 0.03	0.80 ± 0.03	0.81 ± 0.03

Table 1: Table of quantities as a function of the muon P_T threshold.

figure, we see that this corresponds to a P_T^{min2} of approximately 3.5 GeV/c. The $P_T > 3$ GeV/c muon requirement, however, implies a P_T^{min2} of 6.5 GeV. This indicates that the observed portion of the P_T spectrum for the second b is well above any bias introduced by the P_T threshold on the first b. Thus, the electron and muon acceptances may be treated independently.

We generate b quarks, in the range $\mid y_b \mid < 1$, according to partonic distributions provided by MNR. Peterson fragmentation is used to produce B mesons which are decayed according to the IGSW model [7]. We use the MRSB set of structure functions. The systematic uncertainty in the aceptances is obtained by varying the fragmentation parameter and the shape of the b P_T distribution. The fragmentation parameter, ϵ, is varied in the range: $0.004 < \epsilon < 0.008$, corresponding to a 10% variation in acceptance. Varying the shape of the b P_T distribution contributes an additional 15% uncertainty.

Table 1 lists quantities used in calculating the cross section. $A(e)$ is found to be 0.153 ± 0.028. The integrated luminosity of the data is 2.65 ± 0.17 pb^{-1}. The values of χ and the branching fractions are taken to be the world average values :

$\chi = 0.16 \pm 0.04$, $Br(b \rightarrow eX) = 0.107 \pm 0.005$, and $Br(b \rightarrow \mu X) = 0.103 \pm 0.005$ [8]. The values for δ are determined from Monte Carlo.

Figure 3 shows the cross section for $p\bar{p} \rightarrow b\bar{b}X$ and the theoretical prediction from MNR. The cross section is plotted versus the P_T^{min} of the second b given the P_T^{min} of the first b. The inner error bars indicate the size of the statistical uncertainty. The outer error bars represent the combined statistical and systematic uncertainty. The dominant uncertainties are associated with ε_{CUTS} and χ. The theoretical prediction uses the DFLM structure functions and the upper and lower uncertainty bands represent variations in m_b, Λ_4, and μ. The theoretical prediction is seen to be systematically low with respect to the data. The uncertainties in the measurement are highly correlated, tending to change the normalization, but not the shape, of the cross section.

Spatial $b\bar{b}$ correlations are investigated by examining the $\Delta\phi_{e\mu}$ distribution, where $\Delta\phi_{e\mu}$ is the opening angle between the electron and muon in the transverse plane. Figure 4 compares the sign subtracted $\Delta\phi_{e\mu}$ distribution for the data with the MNR prediction. The theoretical prediction is shown both with and without the $M_{e\mu} > 5$ GeV requirement. A rise at low values of opening angle is expected from gluon splitting. The absence of such a rise in the data is seen to be consistent with the effect of the $e\mu$ invariant mass cut.

The data is seen to be consistent with the shape of the $b\bar{b}$ X cross section as predicted by NLO QCD. The absolute normalization of the theoretical prediction is

found to be lower than the data by a factor of 4. The shape of the $\Delta\phi_{e\mu}$ distribution from $b\bar{b}$ production is seen to be in good agreement with the theory.

The authors wish to thank the technical and support staffs of Fermilab and the participating institutions. This work was supported by the U.S. Department of Energy and National Science Foundation, the Italiano Istituto Nazionale di Fisica Nucleare, the Ministry of Science, Culture and Education of Japan, the Natural Sciences and Engineering Research Council of Canada, and the Alfred P. Sloan Foundation.

References

[1] C. Albajar, *et. al.*, Phys. Lett. **B256** (1991).

[2] F. Abe, *et. al.*, Phys. Rev. Lett. **68**, 3403-3407 (1992); F. Abe, *et. al*, Phys. Rev. Lett. **69**, 3704-3708 (1992); F. Ukegawa, *Bottom Quark Production in 1.8 TeV Proton-Antiproton Collisions*, Ph.D. Thesis, University of Tsukuba (1991).

[3] P. Nason, S. Dawson, and R.K. Ellis, Nucl. Phys. **B327** ,49 (1989).

[4] F. Abe *et al*, Nucl. Instrum. Methods Phys. Res., Sect. A **271**, 387 (1988).

[5] R. Hughes, *Reconstruction of B Meson Decays and Measurement of the B Quark and B Meson Production Cross Sections at the Fermilab Tevatron Collider*, Ph.D. Thesis, University of Pennsylvania (1992).

[6] M. Mangano, P. Nason, and G. Ridolfi, Nucl. Phys. **B373** ,295-345 (1992).

[7] N. Isgur, D. Scora, B. Grinstein, and M.B. Wise, Phys. Rev. **D39** (1989).

[8] Particle Data Group, *Review of Particle Properties*, Phys. Lett. **B239** (1990).

Figure Captions

Figure 1: P_T^{rel} for electrons from the data. OS (SS) events are shown in solid (dashed) lines. The difference of the OS and SS distributions is shown with points. The curve is a fit of the sum of the normalized b and c distributions to the subtracted data. The fit yields a value of $1.0^{+0.0}_{-0.1}$ for $f_{b\bar{b}}$, the fraction of the sign-subtracted events from $b\bar{b}$ production.

Figure 2: The MNR prediction for P_T^{min2} (the 90% P_T threshold for b_2) as a function of P_T^{min1}.

Figure 3: The cross section for $p\bar{p} \rightarrow b\bar{b}X$. $M_{c\mu} > 5$ GeV, $\mid y_{b1,2} \mid < 1$. The cross section is plotted as a function of the P_T^{min} of the second b, given the P_T^{min} of the first b. The theoretical prediction and associated uncertainty are represented by the solid and dashed lines, respectively.

Figure 4: The opening angle between the electron and the muon in the transverse plane. The data is shown as dots. The NLO QCD prediction is shown with (solid) and without (dotted) the $M_{c/m\mu} > 5$ GeV requirement. The theoretical prediction including the mass cut is normalized to the data. The theoretical prediction excluding the mass cut is normalized to the data above 80°.

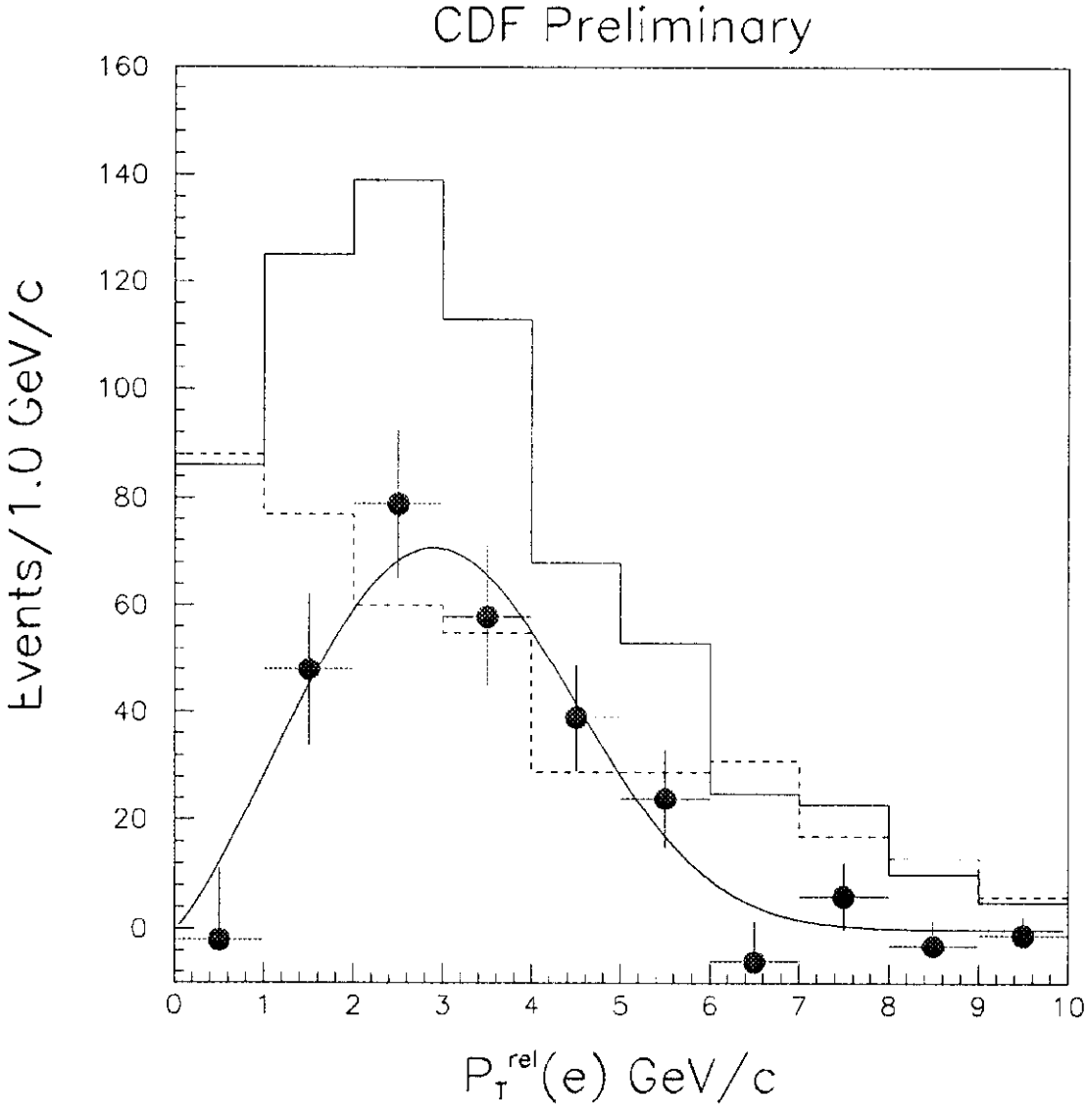
CDF Preliminary
Events/1.0 GeV/c
160
140
120
100
80
60
40
20
0
0
1
2
3
4
5
6
7
8
9
10
$P_T^{rel}(e)$ GeV/c

Figure 1:

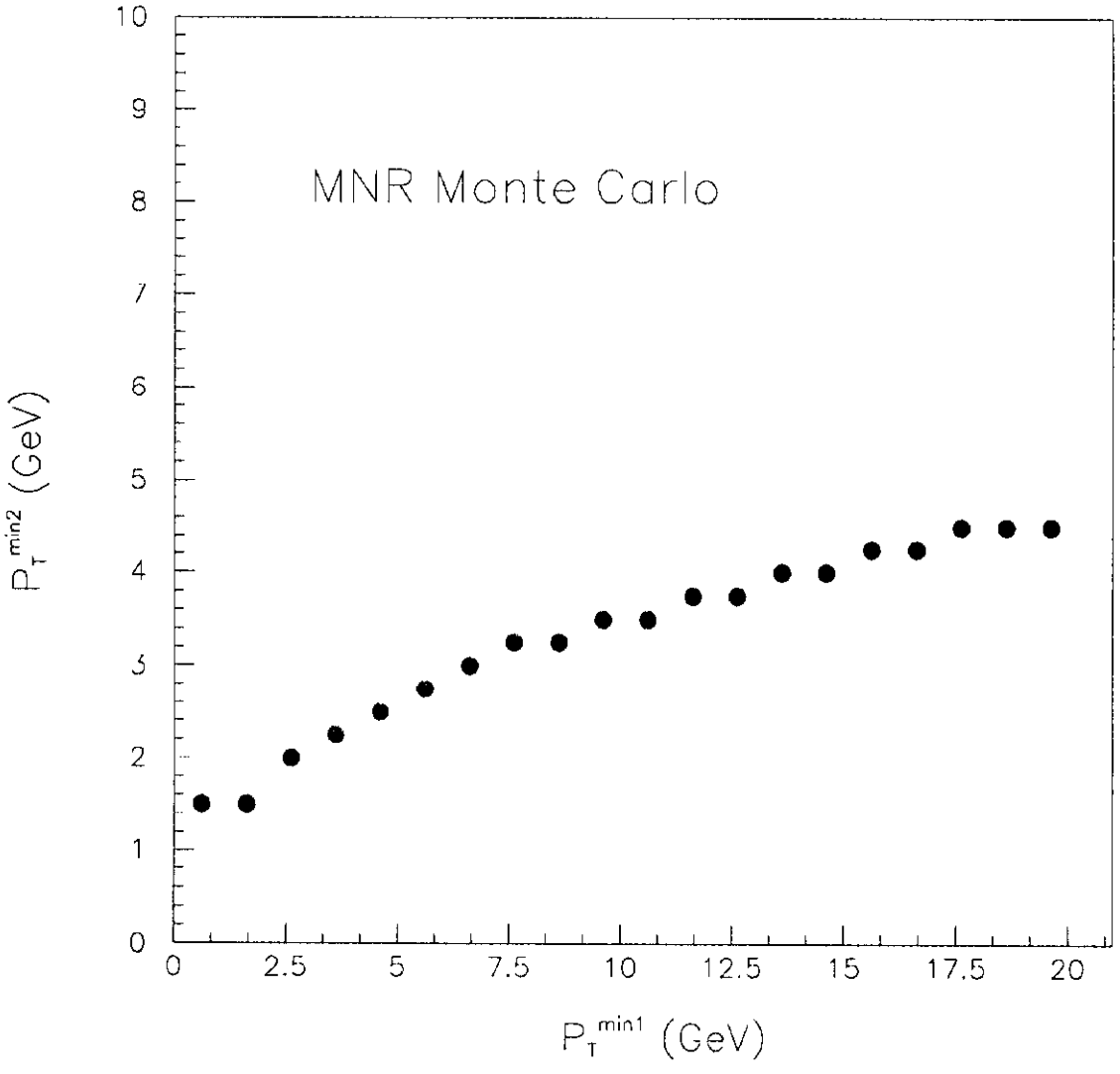
MNR Monte Carlo
P_T^{min2} (GeV)
P_T^{min1} (GeV)
0
1
2
3
4
5
6
7
8
9
10
0
2.5
5
7.5
10
12.5
15
17.5
20

Figure 2:

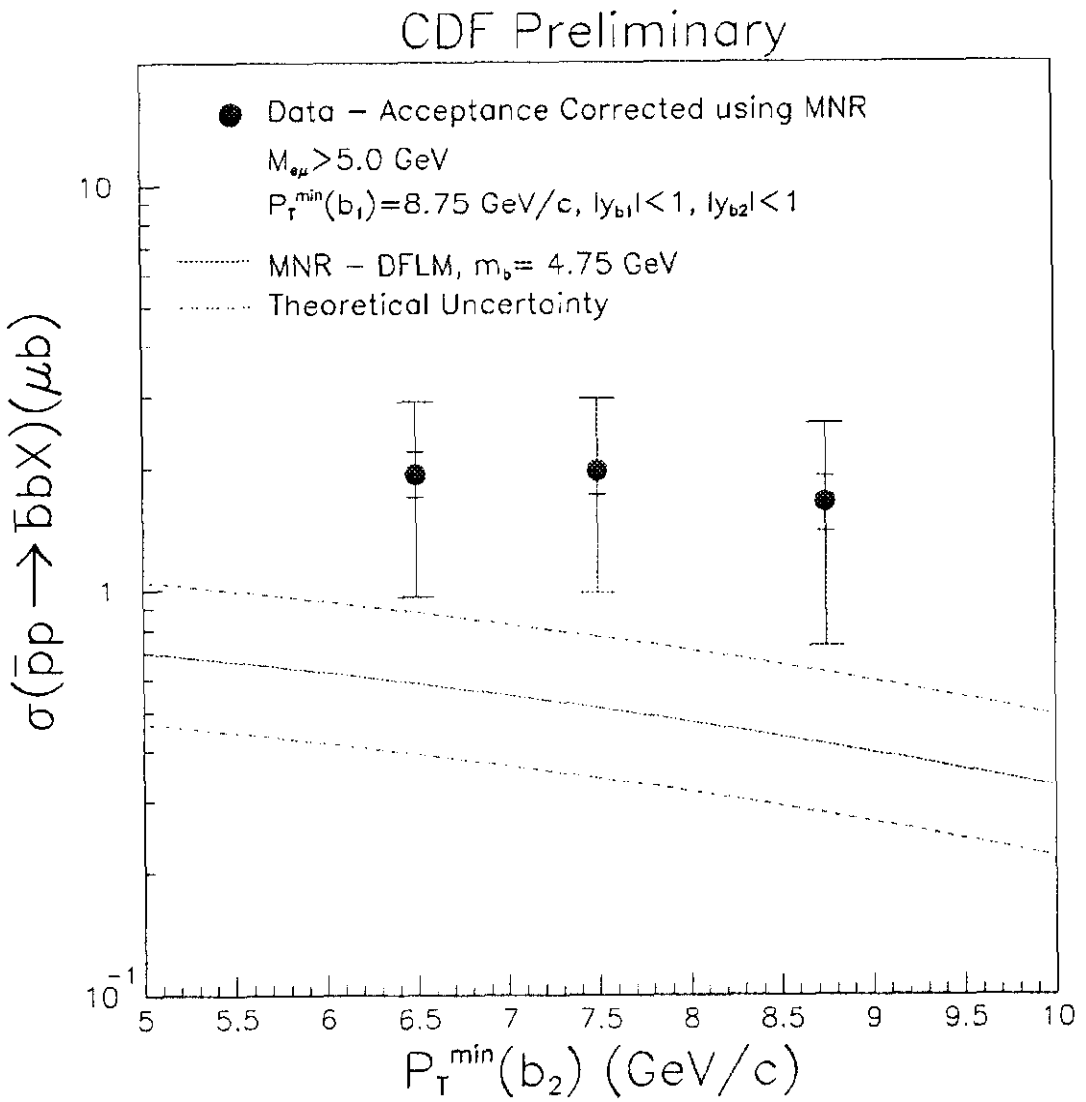
CDF Preliminary
Data – Acceptance Corrected using MNR
$M_{e\mu}$>5.0 GeV
$P_T^{min}(b_1)$=8.75 GeV/c, $|y_{b1}|<1$, $|y_{b2}|<1$
MNR – DFLM, m_b= 4.75 GeV
Theoretical Uncertainty
$\sigma(\bar{p}p \rightarrow b\bar{b}X)(\mu b)$
$P_T^{min}(b_2)$ (GeV/c)
10
1
10^{-1}
5
5.5
6
6.5
7
7.5
8
8.5
9
9.5
10

Figure 3:

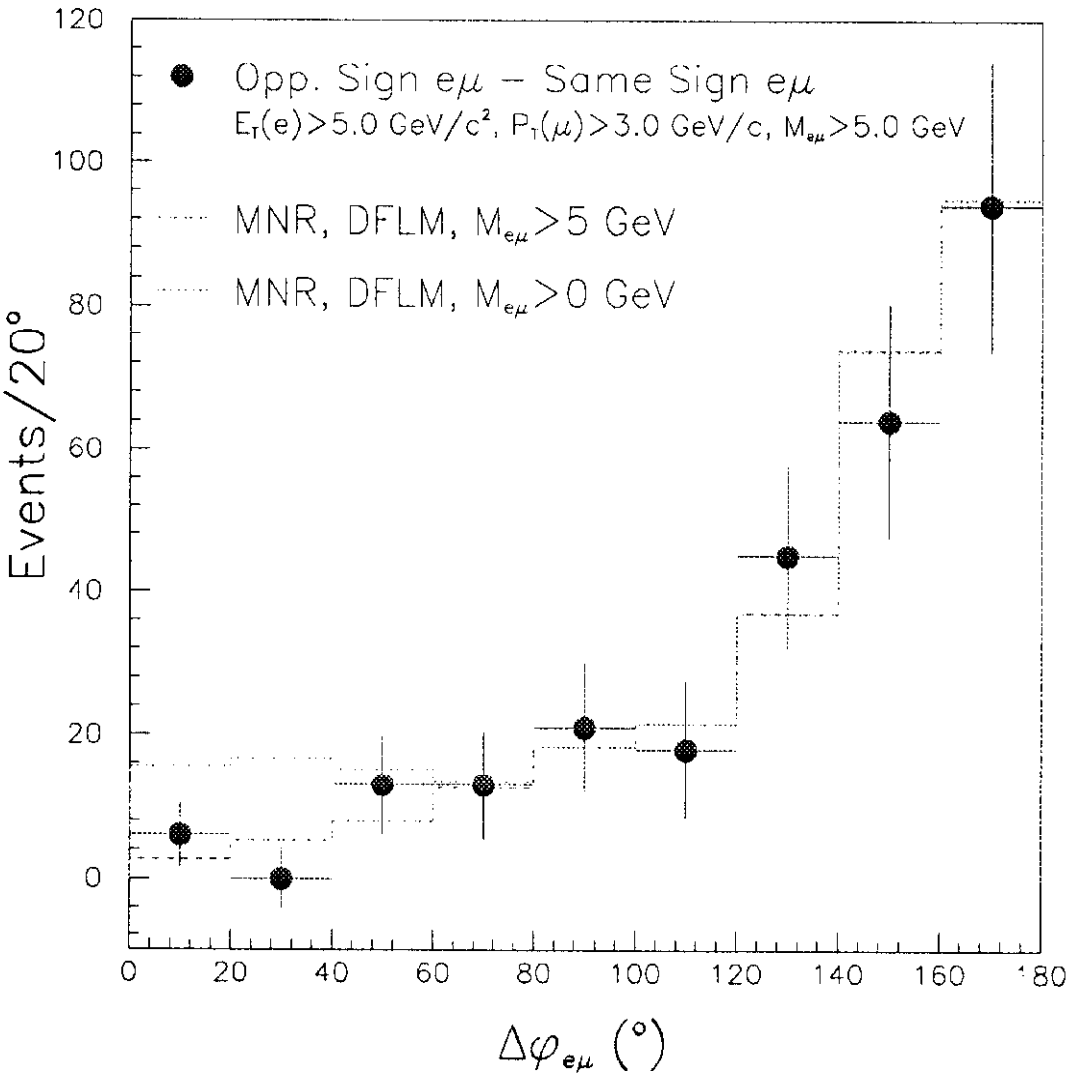
Opp. Sign eμ − Same Sign eμ
E_T(e)>5.0 GeV/c², P_T(μ)>3.0 GeV/c, M_eμ>5.0 GeV
MNR, DFLM, M_eμ>5 GeV
MNR, DFLM, M_eμ>0 GeV
Events/20°
Δφ_eμ (°)
0
20
40
60
80
100
120
140
160
180

Figure 4: